



Synthesis, Characterization and *In vitro* Antitubercular and Antimicrobial Activities of new Aminothiophene Schiff Bases and their Co(II), Ni(II), Cu(II) and Zn(II) Metal Complexes

GANESH MORE¹, SAKINA BOOTWALA^{1*}, SUSHMA SHENOY²,
JOYLINE MASCARENHAS² and K. ARUNA²

¹Department of Chemistry, Wilson College, Mumbai, 400007, India.

²Department of Microbiology, Wilson College, Mumbai, 400007, India.

*Corresponding author E-mail: szbootwala@gmail.com

<http://dx.doi.org/10.13005/ojc/340225>

(Received: October 16, 2017; Accepted: December 25, 2017)

ABSTRACT

Two new clinically active Schiff bases and their transition metal complexes were synthesized and studied by different spectroscopic and physicochemical methods like NMR, IR, UV-visible, ESR, TGA, XRD, mass, elemental analysis, molar conductivity and magnetic susceptibility measurement. Synthesized complexes and Schiff bases were assessed for *In vitro* antituberculosis activity against *Mycobacterium tuberculosis* (ATCC-27294) and for antimicrobial activity against drug resistant (ESBL) Extended Spectrum β -lactamase and (MBL) Metallo β -lactamase producing microbial strains. The biological activity of Schiff base was found to improve in presence of transition metal ions. Among the studied metal complexes, copper complexes displayed superior biological activity against all of the microbial strains.


Keywords: Schiff bases, Antitubercular activity, Antimicrobial activity, Transition metal complex, 2-aminothiophene.

INTRODUCTION

Schiff base being a condensation product of carbonyl compound and primary amine are a subclass of imines, also known as azomethines¹. Over past two decades, Schiff bases are constantly emerging due to ease of preparation and variety in reactions² and enjoyed a popular position in coordination chemistry because of their wide range

of applications from medicinal chemistry to material synthesis³. Azomethine group is an important scaffold critical for biological activity of Schiff bases and present in various natural and non-natural compounds⁴. Schiff bases derived from 2-aminothiophenes derivatives are extensively studied due to their broad spectrum of biological properties and anti-HIV PR inhibitor activities⁵. Schiff base complexes of 3d transition metals were



This is an  Open Access article licensed under a Creative Commons Attribution-NonCommercial-ShareAlike 4.0 International License (<https://creativecommons.org/licenses/by-nc-sa/4.0/>), which permits unrestricted NonCommercial use, distribution and reproduction in any medium, provided the original work is properly cited.

found to exhibit low toxicity and facilitated permeation through the cell membrane of microorganism making them probable therapeutic agents⁶.

Tuberculosis (TB) is one of the giant killers of human history and leading global health hazard of the current century. As per WHO global report of 2015, there were approximately 10.4 million of fresh reported Tuberculosis incidences together with 1.2 million (11%) of HIV-positive cases globally, accounting for approximately 1.4 million TB casualties along with 0.4 million HIV positive casualties⁷. Among the annual TB global estimate, 2.2 million incidences have been reported in India out of which 5% were HIV-positive cases and 2.2% of were multi-drug resistant (MDR) TB cases⁸. The appearance of MDR strains, XDR (extensively drug-resistant) strains and latest TDR (totally drug-resistant) strains with co-infection from HIV virus, made the situation alarming. Thus the treatment becomes costly, involving multiple drugs and of long duration. With an annual global estimate of 250 million cases, (UTIs) urinary tract infections are most frequently confronted diseases in underdeveloped countries⁹. About 35 % of healthy women suffer from symptoms of urinary tract infection once in a lifetime. Most commonly observed cause of UTI is *Escherichia coli*, while few *Gram-positive* bacteria like *Staphylococcus saprophyticus* and *Enterococcus faecalis* and *Gram-negative* uropathogens like *K. pneumoniae*, *P. Aeruginosa*, *Proteus spp.* and *Citrobacter spp.* are also responsible for UTI¹⁰. Random use of antibiotics along with increasing use of invasive diagnostic procedures and lapses in the sterilization has led to the surfacing of antibiotic resistant microorganisms with complex resistance mechanism¹¹ which have made the treatment challenging¹².

Modern studies reported that thiophene containing Schiff bases are strong antibacterial and anti-tubercular agents with potential activity comparable to standard lead compounds¹³⁻¹⁶. Enticed by these results and an extension of our investigation for the new antibacterial and antituberculosis agents¹⁷⁻¹⁹, we have prepared novel Schiff bases and respective transition metal complexes. The present article is focused on

preparation, spectral characterization, and screening of biological activity of these compounds.

EXPERIMENTAL

Methods and materials

Purified and distilled solvents and AR grade chemicals were used in the synthesis. Infra-Red spectrum of the Schiff bases and metal chelates were analyzed using PE 1600 FTIR spectrometer. UV-visible spectra of all compounds were analyzed using Jasco V 630 UV-Vis spectrophotometer in DMF in the region 200–1100 nm. The proton NMR spectra were analyzed on Varian-NMR-Mercury 300 MHz instrument using TMS and DMSO-*d*⁶ as internal standard and solvent respectively. Thermogravimetric analysis of one selected complex was carried out using Perkin Elmer, diamond thermogravimetric analyzer in an inert atmosphere. The elemental analysis and metal percentage were determined by using standard methods²⁰. For magnetic moment measurements, Gouy balance was employed and Mercury(II) Tetrathiocyanatocobaltate(II) was used as a calibration standard. ESR spectra of Cu(II) chelates were analysed under the magnetic field of 3000 Gauss and 9.45 GHz frequency by using JEOL model JES FA200 ESR spectrometer. Mass spectra (MS) were recorded on Bruker Esquire Hct spectrometer. Molar conductance of all compounds was measured on ELICO Ltd. Conductivity meter (Model CM-180) using DMF as solvent at RT.

Preparation of ligand

Ethyl-2-amino-4,5,6,7-tetrahydrobenzo-1-thiophene-3-carboxylate (ETBT) was synthesized using reported method²¹. Schiff base (HL₁ and HL₂) were synthesized from the condensation of ETBT and salicylaldehyde derivatives²² as depicted in Figure. 1.

ETBT

(C₁₁H₁₅NO₂S) m.p: 118 °C; Yield: 85%; LCMS *m/z*: [M]⁺ 225.01; ¹H (300 MHz, DMSO-*d*₆) NMRδ: 7.18 (-NH₂, 2H, s), 4.08-4.15 (-CH₂-, 2H, q), 2.38-2.56 (cyclohexane, 4H, m), 1.63 (cyclohexane, 4H, m), 1.19-1.23 (-CH₃, 3H, t); FTIR (KBr, cm⁻¹): ν_{NH2} 3405, 3301; ν_{C=O} 1648, ν_{C-O} 1274, ν_{C=S} 640; metal content (%) Observed: S 14.20, N 6.21, H 6.66, C 58.59; Calculated: S 13.89, N 6.54, H 6.79, C 58.21.

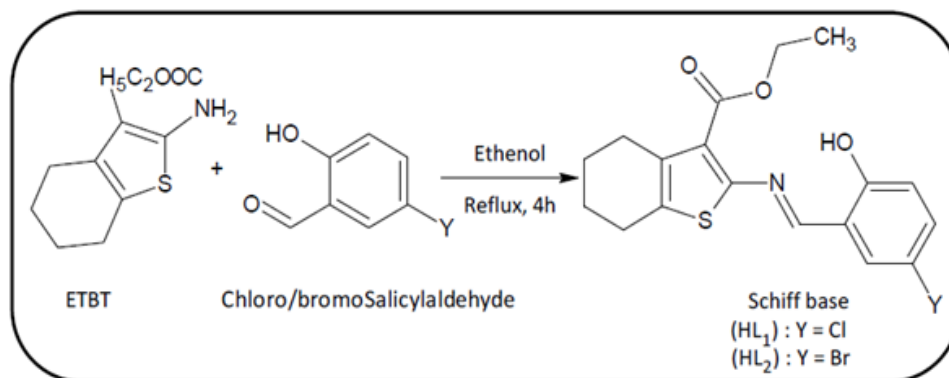


Fig. 1. Reaction scheme

Synthesis of HL₁

The equimolar proportion (0.01 M) of ETBT (2.247 g) and 5-chlorosalicylaldehyde (1.565 g) was taken in dry ethanol and refluxed for 4 hours. The reaction progress was monitored through TLC plates. The yellow product obtained was percolated through filter paper and cleaned with water. It is further purified and allowed to recrystallize in ethanol.

HL₁

(C₁₈H₁₈NO₃SCI) m.p: 123 °C; Yield: 80%; LCMS *m/z*: [M+1]⁺ 364.32; ¹H (300 MHz, DMSO-d₆) NMR δ: 12.53 (-OH, 1H, s), 8.70 (-CH=N-, 1H, s), 4.24-4.31 (-CH₂-, 2H, q), 1.28-1.33 (-CH₃, 3H, m), 6.95-7.73 (aromatic protons of chlorosalicylaldehyde, 3H, m), 2.50-2.69 (aromatic protons of cyclohexane, 4H, m); FTIR (KBr, cm⁻¹): ν_{-OH} 3056, ν_{C=O} 1687, ν_{C=N} 1600, ν_{C-O} 1278, ν_{C=S} 632; metal content (%) Observed: S 7.89, N 3.47, H 4.37, C 52.68; Calculated: S 7.84, N 3.43, H 4.41, C 52.90.

Synthesis HL₂

HL₂ was synthesized by refluxing equimolar proportion (0.01 M) of ETBT (2.247 g) and 5-bromosalicylaldehyde (2.010 g) in ethanol for 4 hours. The orange-yellow product obtained was filtered and cleaned with water and allowed to recrystallize in ethanol.

HL₂

(C₁₈H₁₈NO₃SBr) m.p: 125°C, Yield: 75%, LCMS *m/z*: [M+1]⁺ 409.29, ¹H (300 MHz, DMSO-d₆) NMR δ: 12.55 (-OH, 1H, s), 8.65 (-CH=N-, 1H, s), 4.23-4.30 (-CH₂-, 2H, q), 1.28-1.32 (-CH₃, 3H, m), 6.87-

7.83 (aromatic protons of chlorosalicylaldehyde, 3H, m), 2.50-2.66 (aromatic protons of cyclohexane, 4H, m); FTIR (KBr, cm⁻¹): ν_{-OH} 3056, ν_{C=O} 1687, ν_{C=N} 1600, ν_{C-O} 1278, ν_{C=S} 632; metal content (%) Observed: S 7.89, N 3.47, H 4.37, C 52.68; Calculated: S 7.84, N 3.43, H 4.41, C 52.90.

Synthesis of metal chelates

Cobalt, nickel, copper, and zinc chelates were synthesized by refluxing the ethanolic solution of metal chlorides with warm ethanolic solutions of ligand in 1:1 molar ratio for nickel (II), copper (II) and zinc (II) complexes and in 1:2 molar ratio for cobalt (II) complex at the pH of 6.5 for 6-8 hours. The metal chelates obtained were percolated through filter paper and cleaned with ether and ethanol and dried in vacuum over P₄O₁₀.

[Co(L₁)₂]

CoC₃₆H₃₄N₂O₆S₂Cl₂ (784.63): Yield: 75%, FTIR (KBr, cm⁻¹): ν_{C=O} 1646, ν_{C=N} 1577, ν_{C-O} 1308, ν_{C=S} 633; ν_{Co-O} 510, ν_{Co-N} 412; metal content (%) Observed: Co 7.95, Cl 9.23, S 7.78, N 3.33, H 4.26, C 55.63; Calculated: Co 7.51, Cl 9.04, S 8.16, N 3.57, H 4.33, C 55.06; Molar conductance: 6.00 cm²Ω⁻¹ mol⁻¹

[Ni(L₁)Cl]

NiC₁₈H₁₇NO₃SCI₂ (457.00): Yield: 72%, FTIR (KBr, cm⁻¹): ν_{C=O} 1642, ν_{C=N} 1578, ν_{C-O} 1309, ν_{C=S} 635; ν_{Ni-O} 512, ν_{Ni-N} 410; metal content (%) Observed: Ni 13.26, Cl 15.64, S 6.85, N 3.09, H 3.55, C 47.64; Calculated: Ni 12.84, Cl 15.52, S 7.00, N 3.06, H 3.72, C 47.27; Molar conductance: 3.80 cm²Ω⁻¹ mol⁻¹.

[Cu(L₁)Cl]

$\text{CuC}_{18}\text{H}_{17}\text{NO}_3\text{SCl}_2$ (461.85): Yield: 70%, FTIR (KBr, cm^{-1}): $\nu_{\text{C=O}}$ 1645, $\nu_{\text{C=N}}$ 1574, $\nu_{\text{C-O}}$ 1314, $\nu_{\text{C=S}}$ 635; $\nu_{\text{Cu-O}}$ 520, $\nu_{\text{Cu-N}}$ 418; metal content (%) Observed: Cu 13.41, Cl 15.55, S 7.02, N 2.94, H 3.48, C 46.15; Calculated: Cu 13.76, Cl 15.36, S 6.93, N 3.03, H 3.68, C 46.77; Molar conductance: $4.30 \text{ cm}^2\Omega^{-1} \text{ mol}^{-1}$.

[Zn(L₁)Cl]

$\text{ZnC}_{18}\text{H}_{17}\text{NO}_3\text{SCl}_2$ (463.71): Yield: 74%, FTIR (KBr, cm^{-1}): $\nu_{\text{C=O}}$ 1644, $\nu_{\text{C=N}}$ 1575, $\nu_{\text{C-O}}$ 1309, $\nu_{\text{C=S}}$ 634; $\nu_{\text{Zn-O}}$ 516, $\nu_{\text{Zn-N}}$ 416; metal content (%) Observed: Zn 13.94, Cl 15.71, S 7.14, N 3.12, H 3.15, C 47.12; Calculated: Zn 14.11, Cl 15.29, S 6.90, N 3.02, H 3.67, C 46.58; Molar conductance: $4.60 \text{ cm}^2\Omega^{-1} \text{ mol}^{-1}$.

[Co(L₂)₂]

$\text{CoC}_{36}\text{H}_{34}\text{N}_2\text{O}_6\text{S}_2\text{Br}_2$ (873.54): Yield: 76%, FTIR (KBr, cm^{-1}): $\nu_{\text{C=O}}$ 1650, $\nu_{\text{C=N}}$ 1578, $\nu_{\text{C-O}}$ 1319, $\nu_{\text{C=S}}$ 632; $\nu_{\text{Co-O}}$ 518, $\nu_{\text{Co-N}}$ 406; metal content (%) Observed: Co 6.81, S 7.26, N 3.37, H 3.98, C 50.19; Calculated: Co 6.75, S 7.33, N 3.21, H 3.89, C 49.45; Molar conductance: $2.60 \text{ cm}^2\Omega^{-1} \text{ mol}^{-1}$.

[Ni(L₂)Cl]

$\text{NiC}_{18}\text{H}_{17}\text{NO}_3\text{SBrCl}$ (501.45): Yield: 73%, FTIR (KBr, cm^{-1}): $\nu_{\text{C=O}}$ 1642, $\nu_{\text{C=N}}$ 1575, $\nu_{\text{C-O}}$ 1313, $\nu_{\text{C=S}}$ 632; $\nu_{\text{Ni-O}}$ 513, $\nu_{\text{Ni-N}}$ 407; metal content (%) Observed: Ni 11.53, Cl 7.16, S 6.43, N 2.62, H 3.46, C 43.21; Calculated: Ni 11.70, Cl 7.07, S 6.38, N 2.79, H 3.39, C 43.08; Molar conductance: $2.20 \text{ cm}^2\Omega^{-1} \text{ mol}^{-1}$.

[Cu(L₂)Cl]

$\text{CuC}_{18}\text{H}_{17}\text{NO}_3\text{SBrCl}$ (506.30): Yield: 78%, FTIR (KBr, cm^{-1}): $\nu_{\text{C=O}}$ 1655, $\nu_{\text{C=N}}$ 1576, $\nu_{\text{C-O}}$ 1321, $\nu_{\text{C=S}}$ 633; $\nu_{\text{Cu-O}}$ 514, $\nu_{\text{Cu-N}}$ 411; metal content (%) Observed: Cu 13.05, Cl 7.19, S 6.11, N 2.83, H 3.38, C 41.78; Calculated: Cu 12.55, Cl 7.00, S 6.32, N 2.77, H 3.36, C 42.66; Molar conductance: $1.80 \text{ cm}^2\Omega^{-1} \text{ mol}^{-1}$.

[Zn(L₂)Cl]

$\text{ZnC}_{18}\text{H}_{17}\text{NO}_3\text{SBrCl}$ (508.16): Yield: 72%, FTIR (KBr, cm^{-1}): $\nu_{\text{C=O}}$ 1646, $\nu_{\text{C=N}}$ 1575, $\nu_{\text{C-O}}$ 1310, $\nu_{\text{C=S}}$ 634; $\nu_{\text{Zn-O}}$ 516, $\nu_{\text{Zn-N}}$ 416; metal content (%)

Observed: Zn 12.37, Cl 7.05, S 6.49, N 2.65, H 3.47, C 41.63; Calculated: Zn 12.87, Cl 6.98, S 6.30, N 2.76, H 3.35, C 42.51; Molar conductance: $1.00 \text{ cm}^2\Omega^{-1} \text{ mol}^{-1}$.

**Biological activity assessment
microorganisms**

Extended Spectrum β -lactamase and Metallo β -lactamase producing microorganism namely form the genera, *Escherichia*, *Pseudomonas*, *Citrobacter*, *Klebsiella* and *Proteus* (Table 3) were used for antimicrobial activity assessment. These isolates were collected from suburban hospitals and pathological labs and evaluated for MBL/ESBL characteristics in earlier studies²³. Whereas *M. tuberculosis* - H37Rv strain (ATCC No- 27294) was chosen for *in vitro* antitubercular activity evaluation.

Antimicrobial assessment

The antibacterial activity was assessed by using the agar well-diffusion method²⁴ using DMSO as a solvent. The compounds were tested at a final concentration of 25 $\mu\text{g/ml}$. Actively growing log phase cultures were obtained by inoculating test isolated in BHI (Brain Heart Infusion) broth (10 ml) and incubating it at 37 °C for one day. Muller Hinton agar medium (20 ml) was seeded using 0.4 ml test culture and transferred to each *Petri plate* of 9 cm diameter. The medium was allowed to solidify and then wells were punched using a sterile cork borer on each plate. Test compounds (50 μl) were added to each well and plates were sealed. These plates were kept for incubation for 24 h at 37 °C. Control wells were prepared with 50 μl of DMSO solution. All the observations were made in three sets to report zones of inhibition²⁵.

Antitubercular assessment

Antitubercular assay of all synthesized compounds was carried out using Micro Plate Alamar Blue assay. A standard solution containing 1000 ppm of each compound was prepared. From standard solution, test solutions were prepared in the increasing concentration from 0.8 $\mu\text{g/ml}$ to 100 $\mu\text{g/ml}$. In sterile 96 well plate, mixture of test solution, de-ionized water (200 μl) and Middlebrook 7H9 Broth (100 μl), were taken. This plate was sealed and hatched at 37 °C over a period of five days. Further, 25 μl of Tween 10% and 80% and Almar Blue (1:1 ratio) was dispensed in each well and

incubated for one day. Minimum Inhibitory Concentration (MIC) was reported as pink coloration for the growth of *Mycobacterium* while blue coloration was considered as no bacterial growth in the well²⁶.

RESULTS AND DISCUSSION

Characterization of ligands

Schiff bases were formed by the condensation of ETBT and salicylaldehyde derivative in 1:1 molar proportion. This is supported by the proton NMR spectra recorded in a DMSO-*d*⁶ solvent. In NMR spectra of ligand, two peaks appeared in the range δ 8.65-8.70 ppm assignable to the azomethine proton and second in the range δ 12.53-12.55 ppm for hydroxyl proton. The singlet at 7.18 ppm is due to the primary amino proton of aminothiophene (ETBT) which disappeared confirming the formation of Schiff base. FTIR spectrum of the ligands exhibited absorption bands characteristic of ester carbonyl, azomethine group and the phenolic group at 1687, 1600 and 1278 cm^{-1} respectively. A broad band was observed in the region 3200-3000 cm^{-1} due to the phenolic

group. This value is lower than expected free -OH stretching frequency of 3600-3500 cm^{-1} . This is due to the strong O--H--N type hydrogen bond formation between phenolic -OH, azomethine nitrogen and ester carbonyl forming a kind of bifunctional hydrogen bonding giving rise to two tautomeric forms, phenolimine (i) and quinoneimine (ii). However, as compared to azomethine nitrogen, the ester carbonyl can attract an only scanty share of phenolic -OH. Due to this, the frequency of the ester carbonyl in the ligand spectra is observed relatively higher (1787 cm^{-1}) compared to the free amine (1660 cm^{-1})²². Further, mass spectrum revealed expected molecular ion peaks corresponding to $[M+1]^+$ at m/z 364.32 and 409.29 for Schiff base ligands HL₁ and HL₂ respectively. UV-visible Spectrum of the HL₁ and HL₂ in DMF revealed phenol amine form of the ligand by displaying strong bands due to $n \rightarrow \pi^*$ and $\pi \rightarrow \pi^*$ transitions in the range 27100-31000 cm^{-1} and 40300-40500 cm^{-1} respectively^{22,27}.

Depending on UV-visible, IR, and mass spectrum, phenolamine (i) structure of the Schiff base ligands have been proposed (Figure 2).

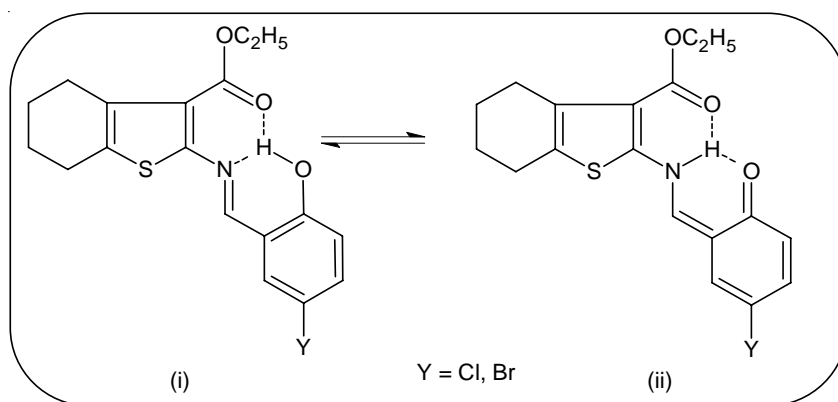


Fig. 2. Tautomeric forms of Schiff base

Structure of the metal chelates

Synthesized complexes were found to be colored with nonhygroscopic properties and stable thermal properties. All metal chelates showed insolubility in normal organic solvents except for DMSO and DMF. C, H, N, S, Cl and metal content of all complexes were found in accordance with the proposed molecular structure. All complexes displayed nonelectrolytic behavior with lower conductance values.

IR spectrum

The FTIR spectrum of ligands and metal chelates in comparison revealed important coordination sites listed in Table 1. Broad band of phenolic group $\nu(\text{OH})$ in the region 3200-3000 cm^{-1} for Schiff base was missing in metal chelate spectra representing bonding of phenolic oxygen with a metal atom. In addition, the transfer of the phenolic oxygen band $\nu(\text{C-O})$ at 1278 cm^{-1} to 1319-1308 cm^{-1} wave regions on chelation supports the

deprotonation of phenolate oxygen. In free ligand, characteristic absorption peaks at 1600 and 1687 cm^{-1} were observed because of azomethine (-CH=N-) and carbonyl ester (-C=O) groups respectively. These absorption bands were downshifted by 20-45 cm^{-1} demonstrating coordination by oxygen of ester carbonyl and nitrogen of azomethine to the metal ion²⁸. This conclusion is favored by the observance of two

non-ligand bands around 418-406 and 520-510 cm^{-1} in metal chelate spectra. These bands may be allocated to $\nu(\text{M}\leftarrow\text{N})$ and $\nu(\text{M}\leftarrow\text{O})$ charge transfer bands respectively. The unaltered position of $\nu(\text{C-S})$ band in the wave region 635-632 cm^{-1} in metal chelate spectra indicates the refraining of thiophene sulphur from the bond formation with the metal atom.

Table 1: Characteristic FTIR peaks

Tentative Assignments	Compounds (cm^{-1})									
	HL ₁	[Co(L ₁) ₂]	[Ni(L ₁)Cl]	[Cu(L ₁)Cl]	[Zn(L ₁)Cl]	HL ₂	[Co(L ₂) ₂]	[Ni(L ₂)Cl]	[Cu(L ₂)Cl]	[Zn(L ₂)Cl]
$\nu(\text{OH})$	3000 -3200					3000 -3200				
$\nu(\text{C=O})$	1687	1646	1642	1645	1644	1687	1650	1642	1655	1646
$\nu(\text{C=N})$	1600	1577	1578	1574	1575	1600	1578	1575	1576	1575
$\nu(\text{C-O})$	1278	1308	1309	1314	1309	1278	1319	1313	1319	1310
$\nu(\text{C-S})$	634	633	635	635	634	632	632	632	632	634
$\nu(\text{M}\leftarrow\text{O})$	-	510	512	520	516	-	518	513	514	516
$\nu(\text{M}\leftarrow\text{N})$	-	412	410	418	416	-	406	407	411	416

UV-visible bands and magnetic moments

In the UV-visible spectrum of the metal chelates, characteristic $\pi\rightarrow\pi^*$ transitions were shifted to a longer wavelength. This shift is because of the LMCT transition indicating chelate formation²⁹. Cobalt complexes exhibited three absorption bands near 24000, 20000 and 10000 cm^{-1} which were ascribed to the ${}^4\text{T}_{1g}(\text{F})\rightarrow{}^4\text{T}_{1g}(\text{P})$ (ν_3), ${}^4\text{T}_{1g}(\text{F})\rightarrow{}^4\text{A}_{2g}(\text{F})$ (ν_2), and ${}^4\text{T}_{1g}(\text{F})\rightarrow{}^4\text{T}_{2g}(\text{F})$ (ν_1), spin allowed transitions respectively. Ligand field splitting parameter (Dq), racah parameter (B), transition ratio (ν_2/ν_1), ligand field stabilization energy (LFSE), and the nephelauxetic ratio (β) were obtained and found within the range of octahedral complexes and are depicted in Table 2. The delocalization of d-orbitals with an orbital overlap of the ligand along with partial covalent bonding between metal and ligand were the observed inference made from the lower B (less than free ion) & β (less than one) values of Co(II) complexes respectively. Magnetic susceptibility values for cobalt complexes were found between 4.83-4.85 BM which supported the octahedral geometry⁶.

The UV-visible spectra of the nickel chelates showed the absence of any band below 10000 cm^{-1} which may be due to the large energy difference between the $d_{x^2-y^2}$ and d_{xy} orbital (>10000 cm^{-1}). The [Ni(L₁)Cl] complex showed bands at 20284 and 24938 cm^{-1} and [Ni(L₂)Cl] complex exhibited band at 20408 and 25000 cm^{-1} , both the bands are due to ${}^1\text{A}_{1g}\rightarrow{}^1\text{A}_{2g}$ and ${}^1\text{A}_{1g}\rightarrow{}^1\text{B}_{1g}$ transitions respectively, which indicate square planer geometry. Both nickel complexes exhibited diamagnetic nature which supported the square planer geometry³⁰. The copper complexes displayed a broad band around 20200 cm^{-1} ascribed to ${}^2\text{B}_{1g}\rightarrow{}^2\text{A}_{1g}$ transition and slightly red-shifted $n\rightarrow\pi^*$ and $\pi\rightarrow\pi^*$ transitions³¹. The [Cu(L₁)Cl] complex exhibited two bands due to $n\rightarrow\pi^*$ and $\pi\rightarrow\pi^*$ transitions at 36900 and 30030

cm^{-1} respectively and one spin allowed ${}^2B_{1g} \rightarrow {}^2A_{1g}$ transition at 20202 cm^{-1} . On the other hand, $[\text{Cu}(\text{L}_2)\text{Cl}]$ complex exhibited three bands at 38023 , 29586 and 19763 cm^{-1} corresponding to $n \rightarrow \pi^*$, $\pi \rightarrow \pi^*$ and ${}^2B_{1g} \rightarrow {}^2A_{1g}$ transition respectively. In addition, $[\text{Cu}(\text{L}_1)\text{Cl}]$ and $[\text{Cu}(\text{L}_2)\text{Cl}]$ complex showed magnetic moment values 1.86 and 1.87 BM

respectively, which supports proposed distorted square-planar geometry. Both zinc are diamagnetic with d^{10} configuration and do not show any d-d transitions. The percentage elemental content is in accordance with the proposed tetrahedral geometry for both the zinc complexes³².

Table 2: Ligand field parameters and magnetic moment of cobalt complexes

Compound	Spectral band (cm^{-1})	Spectral assignment	μ_{eff} BM	(ν_2/ν_1)	Dq (cm^{-1})	B (cm^{-1})	β	LFSE (kJmol^{-1})
$[\text{Co}(\text{L}_1)_2]$	23419	${}^4T_{1g}(\text{F}) \rightarrow {}^4T_{1g}(\text{P})$	4.83	1.94	950.68	848	0.87	76.05
	19607	${}^4T_{1g}(\text{F}) \rightarrow {}^4A_{2g}(\text{F})$						
	10101	${}^4T_{1g}(\text{F}) \rightarrow {}^4T_{2g}(\text{F})$						
$[\text{Co}(\text{L}_2)_2]$	23980	${}^4T_{1g}(\text{F}) \rightarrow {}^4T_{1g}(\text{P})$	4.85	1.98	987.85	907	0.94	79.03
	20000	${}^4T_{1g}(\text{F}) \rightarrow {}^4A_{2g}(\text{F})$						
	10121	${}^4T_{1g}(\text{F}) \rightarrow {}^4T_{2g}(\text{F})$						

Thermogravimetric analysis

Thermogravimetric decomposition of $[\text{Zn}(\text{L}_1)\text{Cl}]$ complexes was studied under an inert atmosphere of nitrogen from room temperature to $1000 \text{ }^\circ\text{C}$. Zinc complex decomposed in two steps as shown in Fig. 3. First TG decomposition peak was observed in the temperature region of $170\text{-}430 \text{ }^\circ\text{C}$ resulting in mass loss of 45.63%

(calculated 45.12%) corresponding to the loss of aminothiophene group. Next, TG decomposition peak was observed around $450\text{-}680 \text{ }^\circ\text{C}$ for mass loss of 37.21% (calculated 37.32%) corresponding to the loss of salicylaldehyde group. Above $700 \text{ }^\circ\text{C}$, only ZnO was left as a residue of observed mass 17.16% (calculated 17.56%).

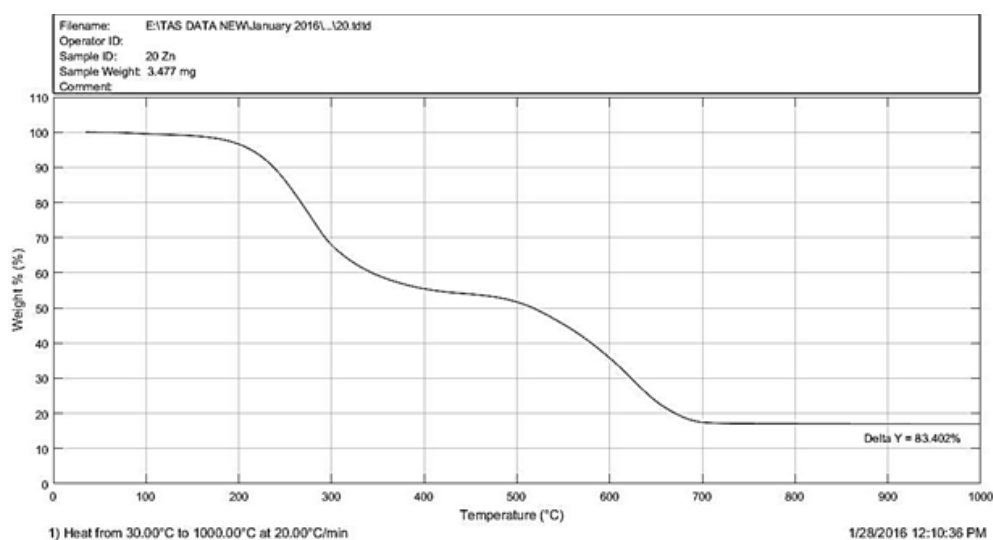


Fig. 3. Thermogram of $[\text{Zn}(\text{L}_1)\text{Cl}]$

EPR spectra

The EPR spectra (X-band) of $[\text{Cu}(\text{L}_1)\text{Cl}]$ at RT was obtained in a solid state which is given in

Fig. 4. The observed ESR parameters were $g_{\parallel} = 2.1467$, $g_{\perp} = 2.0307$, $g_{\text{av}} = 2.0694$ and $A_{\parallel} = 179.6$. The g tensor trending observed $g_{\parallel} > g_{\perp} > g_e$ is

indicative of residence of the unpaired electron inside dx^2-y^2 orbital of copper ion. With the observed g values of the complex, not more than 2.3, substantial covalent nature of the ligand-metal bond can be assumed³³. The factor of axial symmetry $G = (g_{\parallel} - 2/g_{\perp} - 2)$ is 4.77, which indicates the parallel or misalignment of the local tetragonal axes along with negligible exchange interaction. The empirical factor $f = g_{\parallel} / A_{\parallel}$ is frequently used to evaluate tetragonal distortions in tetra-coordinated Cu(II) complexes. The ratio close to 100 indicates square

planer geometry, while 105-135 denotes small to extreme distortion in square planar geometry. The calculated $\mu_{\text{eff}} = 1.79$ and the empirical ratio of 119 observed from ESR spectra, reflects distorted square structure around the Cu(II) ion. Further, molecular orbital coefficient (α^2) was calculated according to Kivelson and Neiman equation, $\alpha^2_{\text{Cu}} = -(A_{\parallel}/0.036) + (g_{\parallel} - 2.002) + 3/7(g_{\perp} - 2.002) + 0.04$. The inplane σ covalency parameter (α^2_{Cu}) for $[\text{Cu}(\text{L}_1)\text{Cl}]$ complex was 0.69, which point towards the covalent character of the metal-ligand bond³⁴.

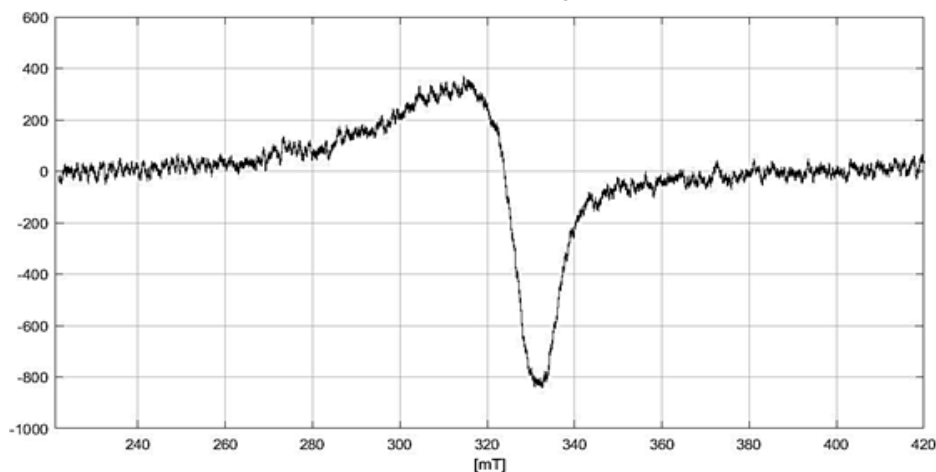


Fig. 4. ESR spectra of $[\text{Cu}(\text{L}_1)\text{Cl}]$ complex

XRD studies

The XRD of the $[\text{Ni}(\text{L}_1)\text{Cl}]$ complex in powder form was obtained in the 2θ range $10^\circ - 90^\circ$ at the wavelength of 1.5406 \AA using $\text{CuK}\alpha$ as the source. The diffractogram presented in Fig. 5, indicated amorphous nature of the complex. Rietveld refinement technique is used to evaluate crystal lattice parameters^{35,36}. The diffractogram

displayed maximum reflection at $2\theta = 22.1270^\circ$ at $d = 4.0141 \text{ \AA}$. The complex showed lattice parameters, $Z = 4$, $V = 3490.72 \text{ \AA}^3$, $a = 17.4800 \text{ \AA}$, $c = 17.4500 \text{ \AA}$ and $b = 11.4440 \text{ \AA}$. The $[\text{Ni}(\text{L}_1)\text{Cl}]$ complex crystallizes in an orthorhombic system with space group $Pca21$ ³⁷. The observed average grain size for the $[\text{Ni}(\text{L}_1)\text{Cl}]$ was 47 nm ³⁸.

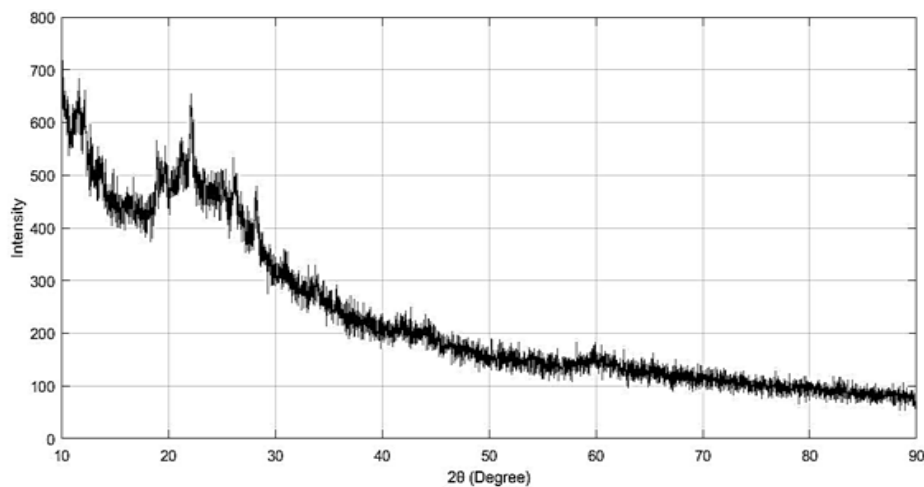


Fig. 5. X-ray diffractogram of $[\text{Ni}(\text{L}_1)\text{Cl}]$ complex

Ligand coordinated to metal ion via azomethine, phenolate, and ester carbonyl group to form metal chelates. On the basis of

spectroscopic and physicochemical techniques, the proposed structures for the metal chelates are shown in Figure 6.

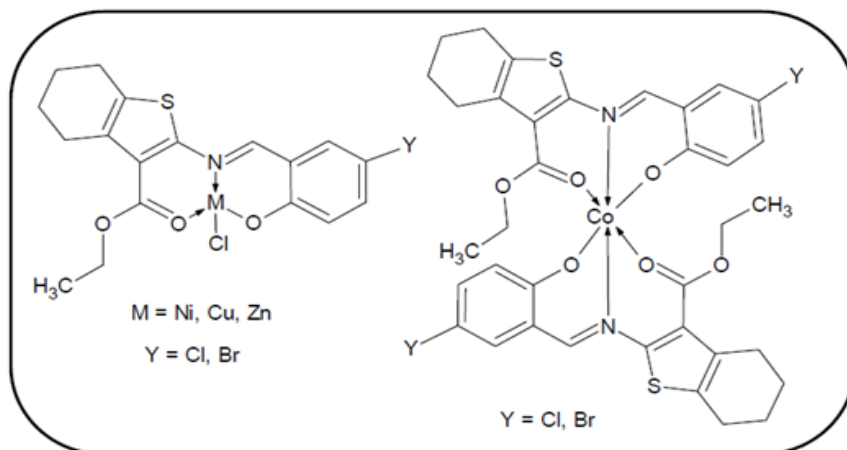


Fig. 6. Proposed configuration of metal chelates

Antimicrobial activity

Multidrug drug-resistant isolates (Table 3) including resistance to 3rd generation cephalosporins were used to carry out a comparative study of antimicrobial activity of *Gram-negative* uropathogens against all synthesized compounds using Kirby Bauer method. The antimicrobial activity of all compounds and DMSO (solvent) in terms of a zone of inhibition (mm) is displayed in Table 4. Metal complexes exhibited higher zones of inhibition than the free ligand except for *P. aeruginosa* and *K. pneumoniae-7* uropathogens, which displayed similar zones of inhibition against ligand as well as their metal complexes. Ligand HL₂ and its transition metal complexes demonstrated higher antimicrobial activity compared to Ligand HL₁ and its transition metal complexes. Copper and zinc complexes were found to be more sensitive as compared to nickel and cobalt complexes and exhibited excellent antimicrobial activity against all test isolates with a zone of inhibition in the range 10-21 mm. Cobalt complex [Co(L₁)₂] displayed zones of inhibition of 11-14 mm except for *K. Pneumonia*, *E. coli-10*, and *P. mirabilis*, which depicted no zone of inhibition. Cobalt complex [Co(L₂)₂] found to be a most active compound with sizeable zones of inhibition (12-21 mm) against most of the microorganism. Nickel complex [Ni(L₁)Cl] displayed substantial zones of inhibition of 11-14 mm except for *C. diversus-2*, *K. pneumoniae* and *P. mirabilis-7*, while [Ni(L₂)Cl] exhibited 10-13 mm zones except for *K.*

pneumoniae, *P. mirabilis-7*, *E. coli* and *P. mirabilis*. All the compounds demonstrated maximum inhibitory activity against *C. amalonaticus* MBL uropathogens with zones of 14-21 mm size, while least antimicrobial activity was observed against *K. pneumoniae* ESBL uropathogens. Compounds [Co(L₂)₂], [Cu(L₂)Cl] and [Cu(L₁)Cl] exhibited significant antimicrobial activity and can be used not only as an approach to enhance their activity but also to overcome the drug resistance.

The enhanced antimicrobial activity of metal chelates in comparison to the ligands may be accredited to the concept of cell permeability and chelation theory. The existence of the electron-withdrawing group in the aromatic ring increases the antimicrobial activity of the metal complex as compared to complex without any substituent³⁹. Liposolubility of the membrane around the microorganism cell controls the course of the lipid-soluble compound. Because of chelation, metal ion shares positive charge on it with the donor group thus reducing polarity of metal ion and increasing the possible delocalization of the (π-electrons over the metal complex ring. This effect increases the lipophilicity of the metal complex and allows efficient infiltration of the metal compound through the lipid membrane to mask the metal coordinating sites on the enzymes of microorganisms, thus reducing the growth of the microorganism. Also, metal chelates were found to

influence the respiration activity of the microorganism by blocking the protein synthesis and hence resulting in cell death and growth restriction of microorganism⁴⁰.

Table 3: Multidrug-resistant microbial cultures

Type of culture	Code name	Biological name
MBL	618	<i>Klebsiella pneumoniae</i>
	607	<i>Proteus mirabilis</i>
	220	<i>Escherichia coli</i>
	135	<i>Citrobacter amalonaticus</i>
	85	<i>Pseudomonas aeruginosa</i>
ESBL	Pro-7	<i>Proteus mirabilis-7</i>
	Kp-7	<i>Klebsiella pneumoniae-7</i>
	Kp	<i>Klebsiella pneumoniae</i>
	Ec-10	<i>Escherichia coli-10</i>
	Citro-2	<i>Citrobacter diversus-2</i>

Table 4: Antimicrobial activity

Sr. No.	Compounds	Zone of Inhibition (mm)									
		ESBL					MBL				
		Citro-2	Ec-10	Kp	Kp-7	Pro-7	85	135	220	607	618
1	DMSO (Solvent)	0	0	0	0	0	0	0	0	0	0
2	HL ₁	0	0	0	11	0	12	14.5	0	0	0
3	[Co(L ₁) ₂]	12	0	0	11	12	12	14	0	0	11
4	[Ni(L ₁)Cl]	0	11	0	11	0	12.5	14	10	10	10
5	[Cu(L ₁)Cl]	16	12	11	10	13	13	16	15	11	10
6	[Zn(L ₁)Cl]	13	12	11	12	11	11.5	18	12	10.5	11
7	HL ₂	0	11	0	12	0	11	14	0	0	10
8	[Co(L ₂) ₂]	20	12	0	12	13	14	21	14	15	16.5
9	[Ni(L ₂)Cl]	10	11	0	12	0	13	13	0	0	10
10	[Cu(L ₂)Cl]	17	13	11	11	15	14	19	17	14	12
11	[Zn(L ₂)Cl]	11.5	13	11	11.5	12	12	17	10	12	11

Antitubercular activity

The antitubercular properties of all prepared compounds were assessed against *M. Tuberculosis* using Streptomycin, Ciprofloxacin and Pyrazinamide standard drugs. All compounds were found active against *M. tuberculosis* as shown in Table 5 and Fig. 7. *M. tuberculosis* is unique due to thick and waxy surrounding cell wall, due to which effective antitubercular drug should be reasonably lipophilic to penetrate the bacterial cell wall⁴¹. Schiff base ligands HL₁ and HL₂ exhibited less activity (MIC=50.0 µg/ml) compared to their metal compounds; this activity can be attributed to the formation of metal chelates, having enhanced lipophilic properties over the Schiff base ligands allowing more efficient permeation of the metal

Table 5: Antitubercular activity

Test compound	MIC (µg/ml)
Pyrazinamide*	3.12
Ciprofloxacin*	3.12
Streptomycin*	6.25
HL ₁	50.0
[Co(L ₁) ₂]	50.0
[Ni(L ₁)Cl]	25.0
[Cu(L ₁)Cl]	12.5
[Zn(L ₁)Cl]	12.5
HL ₂	50.0
[Co(L ₂) ₂]	25.0
[Ni(L ₂)Cl]	25.0
[Cu(L ₂)Cl]	12.5
[Zn(L ₂)Cl]	25.0

* Standard

complex through the thick microbial cell wall leading to better antitubercular activity⁴⁰. Copper complexes were most active against *M. tuberculosis* compared to cobalt, nickel and zinc complexes. Copper

complex $[\text{Cu}(\text{L}_2)\text{Cl}]$ and $[\text{Cu}(\text{L}_1)\text{Cl}]$ and zinc complex $[\text{Zn}(\text{L}_1)\text{Cl}]$ exhibited high antitubercular activity, while Cobalt and Nickel complexes exhibited reasonable antitubercular activity.

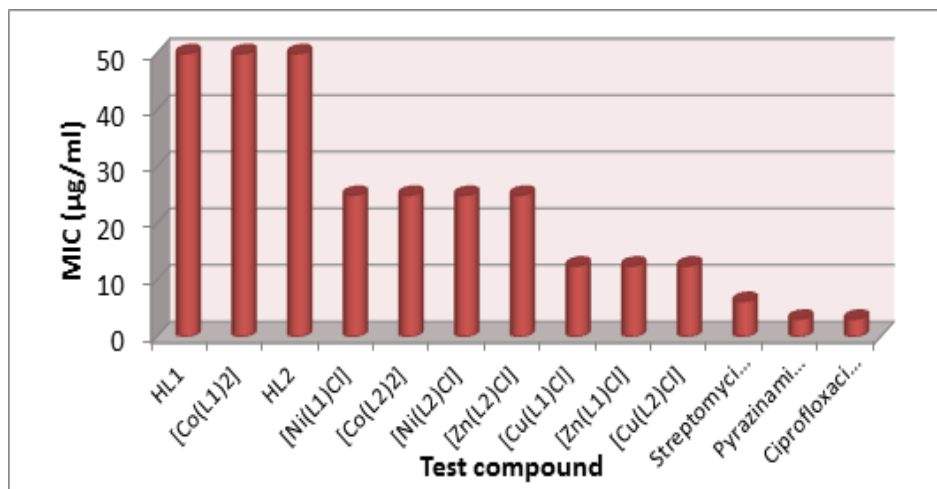


Fig. 7. Antitubercular activity profile

CONCLUSION

Transition metal complexes and two new Schiff bases were prepared. These compounds were evaluated by various spectroscopic techniques. The physical and spectral data revealed monobasic tridentate nature of Schiff base and ligand to metal ratio of 2:1 for cobalt complex and 1:1 for copper, zinc and nickel chelates. Octahedral arrangement for cobalt complexes, square planar geometry for nickel complexes, the distorted square planar configuration for copper complexes and tetrahedral geometry for zinc complexes have been predicted. The biological activity studies revealed the higher antibacterial and antitubercular activity of metal chelates compared to parent ligand against ESBL and MBL uropathogens and *M. Tuberculosis*.

Copper complex $[\text{Cu}(\text{L}_2)\text{Cl}]$ and $[\text{Cu}(\text{L}_1)\text{Cl}]$ and cobalt complex $[\text{Co}(\text{L}_2)_2]$ complexes exhibited significant antimicrobial activity, while copper complex $[\text{Cu}(\text{L}_2)\text{Cl}]$ and $[\text{Cu}(\text{L}_1)\text{Cl}]$ and zinc complex $[\text{Zn}(\text{L}_1)\text{Cl}]$ complexes demonstrated high anti-tubercular activity. This research work could provide the possibility of synthesizing new lead compounds with more active therapeutic properties that can be used as potential metal derived drugs.

ACKNOWLEDGEMENT

The authors thank MMNGH Dental College, Belgaum for facilitating anti-TB activity and IIT SAIF, Bombay, for spectral analysis. Authors also thank Dr. M Mandewale for the necessary help.

REFERENCES

1. Cohen, A.B., The interaction of α -1-antitrypsin with chymotrypsin, trypsin and elastase, *Biochimica et Biophysica Acta (BBA)-Enzymology.*, **1975**, *391*(1), 193-200.
2. Mishra, N., Poonia, K., Kumar, D., An overview of biological aspects of Schiff base metal complexes, *Int. J. Adv. Res. Tech.*, **2013**, *2*(8), 52-66.
3. Brodowska, K., E. Lodyga-Chruścińska., Schiff bases-interesting range of applications in various fields of science, *Chemik.*, **2014**, *68.2*, 129-134.
4. Al Zoubi, W., Biological activities of Schiff bases and their complexes: a review of recent works, *Int. J. Org. Chem.*, **2013**.
5. Souza, B., De Oliveira, T., Aquino, T., de Lima, M., Pitta, I., Galdino, S., Lima, E., Gonçalves-Silva,

- T., Militão, G., Scotti, L. and Scotti, M., Preliminary antifungal and cytotoxic evaluation of synthetic cycloalkyl [b] thiophene derivatives with PLS-DA analysis, *Acta Pharmaceutica*, **2012**, *62*(2), 221-236.
6. Singh, K., Thakur, R., Kumar, V., Co (II), Ni (II), Cu (II), and Zn (II) complexes derived from 4-[[3-(4-bromophenyl)-1-phenyl-1H-pyrazol-4-ylmethylene]-amino]-3-mercapto-6-methyl-5-oxo-1, 2, 4-triazine, *Beni-Suef Univ. J. Basic Appl. Sci.*, **2016**, *5*(1), 21-30.
 7. World Health Organization, Global Tuberculosis Report, **2016**, http://www.who.int/tb/publications/global_report/gtbr2016_executive_summary.pdf?ua=1
 8. TB India, Revised National TB Control Programme Annual Status Report, **2016**. <http://tbcindia.nic.in/showfile.php?lid=3180>
 9. Beyene, G., Tsegaye, W., Bacterial uropathogens in urinary tract infection and antibiotic susceptibility pattern in jimma university specialized hospital, southwest Ethiopia, *Ethiop. J. Health Sci.*, **2011**, *21*(2), 141-146.
 10. Haque, R., Akter, M.L., Salam, M.A., Prevalence and susceptibility of uropathogens: a recent report from a teaching hospital in Bangladesh, *BMC research notes*, **2015**, *8*(1), 416.
 11. Oberoi, L., Singh, N., Sharma, P., Aggarwal, A., ESBL, MBL and Ampc β lactamases producing superbugs-Havoc in the intensive care units of Punjab India, *J. Clin. Diagn. Res.*, **2013**, *7*(1), 70-3.
 12. Deshmukh, D.G., Damle, A.S., Bajaj, J.K., Bhakre, J.B., Patwardhan, N.S., Metallo- β -lactamase-producing clinical isolates from patients of a tertiary care hospital, *J. Lab. Physicians*, **2011**, *3*(2), 93.
 13. Nallangi, R., Samala, G., Sridevi, J.P., Yogeewari, P., Sriram, D., Development of antimycobacterial tetrahydrothieno[2,3-c]pyridine-3-carboxamides and hexahydrocycloocta[b]thiophene-3-carboxamides: molecular modification from known antimycobacterial lead, *Eur. J. Med. Chem.*, **2014**, *76*, 110–117.
 14. Aboul-Fadl, T., Bin-Jubair, F.A., Aboul-Wafa, O., Schiff bases of indoline-2, 3-dione (isatin) derivatives and nalidixic acid carbohydrazide, synthesis, antitubercular activity and pharmacophoric model building, *Eur. J. Med. Chem.*, **2010**, *45*(10), 4578-4586
 15. Ünver, Y., Sancak, K., Celik, F., Birinci, E., Küçük, M., Soyulu, S. Burnaz, N.A., New thiophene-1, 2, 4-triazole-5 (3)-ones: Highly bioactive thiosemicarbazides, structures of Schiff bases and triazole–thiols, *Eur. J. Med. Chem.*, **2014**, *84*, 639-650.
 16. Srivastava, S., Das, B., Synthesis and evaluation of some novel thiophenes as potential antibacterial and mycolytic Agents, *Der Pharma Chemica*, **2011**, *3*(6), 103-111.
 17. More, G., Raut, D., Aruna, K., Bootwala, S., Synthesis, spectroscopic characterization and antimicrobial activity evaluation of new tridentate Schiff bases and their Co (II) complexes, *J. Saudi Chem. Soc.*, **2017**. DOI: <https://doi.org/10.1016/j.jscs.2017.05.002>
 18. Aruna, K., Tariq, M., Bootwala, S., More, G., Cadmium and mercury complexes of a Schiff base ligand: Synthesis, spectral characterization, thermal and antimicrobial properties, *IJPRBS*, **2014**, *3*(5), 222-236.
 19. Aruna, K., Tariq, M., Bootwala, S., More, G., Palladium and platinum complexes of 2-amino-N'-[(1E,2Z)-2-(hydroxyimino)-1-phenylethylidene]-4, 5, 6, 7-tetrahydro-1 benzothiophene-3-carbohydrazide: synthesis, structure, spectral properties and antimicrobial activity, *WJPPS*, **2014**, *3*(10), 784–793.
 20. Vogel Al., Textbook of quantitative chemical analysis, *London: Longmans, Addison Wesley*, **1999**.
 21. Gewald, K., Schinke, E., Bottcher, H., *Chem. Berr.*, **1966**, *99*, 94-100.
 22. Devi, S.N., Mohanan, K., Manganese (II), iron (II), cobalt (II), nickel (II) and zinc (II) complexes of 2-(N-salicylideneamino)-3-carboxyethyl-4,5,6,7 tetrahydrobenzothiophene, *Asian J. Chem.*, **2002**, *14.3*, 1678-1682.
 23. Tariq, M., Aruna, K., Phenotypic and Molecular characterization of MBL genes among uropathogens isolated in Mumbai city, *Br. Microbiol. Res. J.*, **2015**, *5.4*, 368-383.
 24. Aruna, K., Mobashshera, T., Prevalence of extended spectrum beta-lactamase production among uropathogens in South Mumbai and its antibiogram pattern, *Excli J.*, **2012**, *11*, 363.
 25. Ahmad, I., Beg, A.Z., Antimicrobial and phytochemical studies on 45 Indian

- medicinal plants against multi-drug resistant human pathogens, *J. Ethnopharmacol.*, **2001**, *74*(2), 113-123.
26. Lourenço, M. C., de Souza, M. V., Pinheiro, A. C., Ferreira, M. D. L., Gonçalves, R. S., Nogueira, T. C. M., Peralta, M. A., Evaluation of anti-tubercular activity of nicotinic and isoniazid analogues, *Arxivoc*, **2007**, *15*, 181-191.
 27. Kumar, R.N., Chauhan, N.M., Das, A.K., Singh, S.K., Characterization of (2+ 2) Macrocyclic Compounds of Co (II) and Ni (II) Derived from 2, 6-Diacetyl Pyridine and PhenyleneDiamines, *Asian J. Chem.*, **2000**, *12*(2), 428.
 28. Ramasubramanian, A.S., Bhat, R.B., Dileep, R., Rani, S., Transition metal complexes of 5-bromosalicylidene-4-amino-3-mercapto-1,2,4-triazine-5-one: Synthesis, characterization, catalytic and antibacterial studies, *J. Serb. Chem. Soc.*, **2011**, *76*(1), 75-83.
 29. Jamil, W., Solangi, S., Ali, M., Khan, K.M., Taha, M., Khuhawar, M.Y., Syntheses, characterization, in vitro antiglycation and DPPH radical scavenging activities of isatinsalicylhydrazidehydrazone and its Mn (II), Co (II), Ni (II), Cu (II), and Zn (II) metal complexes, *Arab. J. Chem.*, **2015**. DOI: <https://doi.org/10.1016/j.arabjc.2015.02.015>
 30. Ray, R., K., Electronic Spectra of Transition Metal Complexes, *New Central Book Agency (P) Ltd, Kolkata*, **2011**, 387.
 31. Al-Shaalan, N.H., Synthesis, characterization and biological activities of Cu (II), Co (II), Mn (II), Fe (II), and UO₂ (VI) complexes with a new Schiff base hydrazone: O-Hydroxyacetophenone-7-chloro-4-quinoline hydrazone, *Molecules*, **2011**, *16*(10), 8629-8645.
 32. Bootwala, S.Z., Synthesis, Spectroscopic Characterization and Thermal Study of Some Transition Metal Complexes of 2-Amino-*N'*-[(1*E*, 2*Z*)-2-(hydroxyimino)-1-phenylethylidene]-4, 5, 6, 7-tetrahydro-1-benzothiophene-3-carbohydrazide, *Asian J. Chem.*, **2012**, *24*(9), 3849.
 33. Bootwala, S., Tariq, M., Somasundaran, S., Aruna, K., Synthesis, Spectroscopic and Biological Characterization of Some Transition Metal Complexes with Ethyl 2-[[*(2E, 3 Z)*-4-Hydroxypent-3-*En*-2-Ylidene] Amino]-4, 5, 6, 7-Tetrahydro-1-Benzothiophene-3-carboxylate, *IJPBS*, **2013**, *3*(3), 345-354.
 34. Sawant, D.C., Deshmukh, R.G., Structural studies of Co (II), Ni (II), Cu (II) and Zn (II) complexes of *N''*-[(1*Z*, 2*E*)-2-(hydroxyimino)-1-phenylpropylidene]-*N''*-[(1*E*) phenylmethylene] thiocarbonohydrazide, *J. Chem. Pharm. Res.*, **2011**, *3*(6), 464-477.
 35. Rietveld, H., A profile refinement method for nuclear and magnetic structures, *J. Appl. Cryst.*, **1969**, *2*(2), 65-71.
 36. Warren, B.E., X-ray Diffraction, *Dover, New York*, **1990**, 253.
 37. Khan, M. I., Nome, R. C., Deb, S., McNeely, J. H., Cage, B., Doedens, R. J., Inorganic Organic Hybrid Materials with Novel Framework Structures: Synthesis, Structure, and Magnetic Properties of [Ni(py)₄]₂V₁₀O₂₉ and [Ni₂(py)₅(H₂O)₃]₄V₄O₁₂, *Cryst. Growth Des.*, **2009**, *9*(6), 2848-2852.
 38. Kavitha, P., Chary, M.R., Singavarapu, B.V.V.A., Reddy, K.L., Synthesis, characterization, biological activity and DNA cleavage studies of tridentate Schiff bases and their Co (II) complexes, *J. Saudi Chem. Soc.*, **2016**, *20*(1), 69-80.
 39. Sheikh, J., Juneja, H., Ingle, V., Ali, P., Hadda, T.B., Synthesis and in vitro biology of Co (II), Ni (II), Cu (II) and Zinc (II) complexes of functionalized beta-diketone bearing energy buried potential antibacterial and antiviral O, O pharmacophore sites, *J. Saudi Chem. Soc.*, **2013**, *17*(3), 269-276.
 40. Yamgar, R.S., Nivid, Y., Nalawade, S., Mandewale, M., Atram, R.G., Sawant, S.S., Novel zinc (II) complexes of heterocyclic ligands as antimicrobial agents: synthesis, characterisation, and antimicrobial studies, *Bioinorg. Chem. Appl.*, **2014a**. DOI: <http://dx.doi.org/10.1155/2014/276598>
 41. Lu, X., Wan, B., Franzblau, S.G., You, Q., Design, synthesis and anti-tubercular evaluation of new 2-acylated and 2-alkylated amino-5-(4-(benzyloxy) phenyl) thiophene-3-carboxylic acid derivatives. Part 1, *Eur. J. Med. Chem.*, **2011**, *46*(9), 3551-3563.